



Article

Radical Species Production and Color Change Behavior of Wood Surfaces Treated with Suppressed Photoactivity and Photoactive TiO₂ Nanoparticles

Vicente Hernandez ^{1,2,*}, Constanza Morales ², Nicole Sagredo ², Gabriel Perez-Gonzalez ^{2,3}, Romina Romero ⁴  and David Contreras ^{2,3} 

¹ Facultad de Ciencias Forestales, Universidad de Concepción, Victoria 631, Concepción 40730386, Chile

² Centro de Biotecnología, Universidad de Concepción, Barrio Universitario S/N, Concepción 40730386, Chile; conmorales@udec.cl (C.M.); nsagredonh@gmail.com (N.S.); gperezg90@gmail.com (G.P.-G.); dcontrer@udec.cl (D.C.)

³ Facultad de Ciencias Químicas, Universidad de Concepción, Edmundo Larenas 129, Concepción 4070371, Chile

⁴ Laboratorio de Investigaciones Medioambientales de Zonas Áridas (LIMZA), Depto. Ingeniería Mecánica, Facultad de Ingeniería, Universidad de Tarapacá, Arica 100001, Chile; rominaromero@udec.cl

* Correspondence: vhernandezc@udec.cl; Tel.: +56-41-2661449

Received: 8 October 2020; Accepted: 26 October 2020; Published: 27 October 2020



Abstract: The use of TiO₂ nanoparticles for photoprotection comprise a side effect due to the photocatalysis of the nanoparticles under UV radiation. In this work we studied how the suppression of TiO₂ photocatalytic activity may affect the production of phenoxy radicals and the color of wood surfaces exposed to UV radiation. The experimental work considered the modification of TiO₂ nanoparticles to reduce its photoactivity and the use electron paramagnetic resonance to test free radical production. Wood samples were treated with the different TiO₂ nanoparticles and the radical production and color changes were evaluated after UV exposure. Experimental results showed that in wood samples exposed to UV radiation the use of TiO₂ with suppressed photoactivity yielded increased amounts of phenoxy radicals, in comparison to samples treated with photoactive TiO₂. Similar results were obtained in terms of color change, where samples treated with suppressed photoactivity TiO₂ showed significantly higher color changes values, after 2000 h of UV exposure, than samples treated with photoactive TiO₂. These results suggest that in wood surfaces, the photocatalytic effect of TiO₂ may be crucial on the performance of the nanoparticles as photoprotective treatment.

Keywords: free radicals; photocatalysis; TiO₂; UV radiation; wood photodegradation; wood surface color change

1. Introduction

The use of TiO₂ nanoparticles (NP) has resulted in important technological advances for material protection. In wood surfaces, which are highly susceptible to photodegradation, the use of TiO₂ NP is effective at reducing color changes due to photodegradation when applied directly onto the surface or in combination with coating systems [1,2]. The effectiveness of TiO₂ as a photoprotective treatment is related to its ability to block, scatter and absorb UV radiation [3]. UV radiation can break down carbon–carbon, carbon–oxygen and carbon–hydrogen bonds present in the different polymers that form part of wood, inducing undesirable color changes due to photo-oxidative reactions [4].

At nano-scale, the absorption of UV radiation by TiO₂ comprises a complex process in which highly reactive radical species are produced in the presence of oxygen and water [5–9]. The inherent

potential of these radical species to induce chemical changes have drawn concerns on the secondary effect of photoprotective treatments with photocatalysts such as TiO_2 [10–12]. For instance, it has been suggested that inorganic photo-sensitizers may generate reactive oxygen species (ROS) that can contribute to the discoloration of wood [13,14]. Similarly, hydroxy radicals (OH), which are produced during the photocatalysis of TiO_2 , are also involved in the photo-oxidative process of wood and have been reported during the first stages of wood decay [15,16]. Despite the conditions for photocatalysis in wood surfaces treated with TiO_2 NP being present during natural and artificial exposure to UV, color changes or damage attributable to photocatalysis are rarely reported, hence the question about the role played by the photocatalytic effect of TiO_2 on the protection of wood surfaces against UV radiation.

In polymeric films, the suppression of TiO_2 NP photocatalytic activity has resulted in improved photoprotection and increased lifetime of the product; such an effect can be achieved by the addition of a mineral layer onto the surface of the nanoparticles [3]. In this work, we studied how the suppression of the photocatalytic activity of TiO_2 NP may affect its photoprotective action against UV radiation on wood surfaces. The study considered the modification of highly photoactive rutile TiO_2 NP with tetraethyl orthosilicate (TEOS) to generate a silica cover aimed to prevent the interaction of free radicals with the substrate. Modified and unmodified TiO_2 NP were studied on the ability to produce $\cdot\text{OH}$ radicals in vitro by using spin-trapping electron paramagnetic resonance (EPR) spectroscopy. The nanoparticles were then impregnated into small wood samples, and after irradiation with UV light, EPR spectroscopy was used to study the presence of phenoxy radicals. These radicals are readily produced in wood due to the photolysis of lignin in presence of UV radiation [17]. Finally, in a different experiment, the color change in wood surfaces treated with modified and unmodified TiO_2 NP was evaluated after a long-term exposure to UV radiation.

2. Materials and Methods

2.1. Nanoparticles

TiO_2 NP, rutile 99% purity, was purchased from US Research Nanomaterials, Inc. According to the manufacturer the nanoparticles had white appearance, almost spherical morphology, a size of 100 nm and a density of 4.23 g/cm^3 . TiO_2 NP with reduced photocatalytic activity were produced by using the method proposed by Chia and Leong [18]. The procedure consists on the deposition of a silica layer onto the surface of the NP, which prevent the migration of free radical from the NP to the substrate in condition of UV irradiation. In brief, 26 mg of TiO_2 NP were dispersed in 60 mL of ethanol/isopropanol (2:1; *v/v*, Merck, Darmstadt, Hesse, Germany). Then 5 mL of nano-pure water and 1.5 mL of NH_3 (28%, Merck) were added to dispersion. The obtained dispersion was sonicated for 30 min, at room temperature, and in the following 8 h 400 μL of tetraethyl orthosilicate (TEOS, Sigma-Aldrich, St. Louis, MO, USA) were added under stirring conditions. The resultant product, called TiO_2 -Si NP, was centrifuged (6000 rpm) for 10 min and the supernatant discarded. TiO_2 -Si NP were then washed with nano-pure water and dried at room temperature. All reagents were technical degree and were used without further purification.

2.2. Photoactivity Tests on Nanoparticles

TiO_2 NP and TiO_2 -Si NP were tested on their photocatalytic activity by using a Bruker EMX micro with ER 4119HS cavity, electron paramagnetic resonance (EPR) equipment. The EPR device was used to assess the kinetic of abducted $\cdot\text{OH}$ radicals intensity during 50 min of direct irradiation with artificial UV light 340 nm. Experiments considered the addition of $1.23 \times 10^{-4} \text{ mol}$ of active NP in 2.5 mL of 5,5-Dimethyl-1-pyrroline N-oxide (DMPO, Sigma-Aldrich) ($0.01 \text{ mol}\cdot\text{L}^{-1}$). After that the dispersion was sonicated and exposed to UV light under stirring. Aliquots were taken from the dispersion almost every minute during the first ten minutes of the test, and then every ten minutes until complete 60 min. Obtained aliquots were injected into the EPR equipment to perform the measure of OH radicals intensity. In these experiments the magnetic field was adjusted to the dominant peaks

of the adduct spectrum, and the change in the absorption at this field was used as a measure of the concentration of the adduct and thereby of the OH radicals. The amount of DMPO/OH produced is proportional to the height of this peak [19].

In a separate experiment, wood splinters ($1 \times 1 \times 10 \text{ mm}^3$) were prepared from the sapwood portion of a radiata pine board, previously oven dried to 12% moisture content. The splinters were immersed for 5 h in either TiO_2 NP or TiO_2 -Si NP ethanol dispersions (1%), under stirring, and then collected and dried at room temperature for 24 h. Nanoparticles impregnated wood splinters were subsequently exposed to artificial UV radiation, 340 nm for 120 min and inserted in the EPR cavity to measure the intensity of free radicals produced.

In both experiments, EPR measurement were conducted at a microwave power of 2000 mW, frequency modulation of 100 kHz, the center field was fixed at 3515 G with a sweep width of 200 G. The receiver gain was set at 20 dB with a sweep time of 30 s.

2.3. Application of Nanoparticles on Wood Surfaces

A factorial experiment was prepared to test the effect of TiO_2 NP and TiO_2 -Si NP on the surface of radiata pine samples. In the experiment radiata pine samples ($n = 3$) were prepared from 12% moisture content wood boards, without defects. The samples were cut and planed to $10 \times 40 \times 80 \text{ mm}^3$ with their grain longitudinally oriented. Dispersion of TiO_2 NP and TiO_2 -Si NP were prepared in ethanol to a concentration of 1%, respectively, and then applied onto the samples in four consecutive layers by brushing. The experiment considered the application of one type of nanoparticle per samples, plus control samples without treatment. Treated and control samples were dried at room temperature for 24 h, prior to their exposure to UV radiation.

2.4. UV Exposure

Treated and control wood samples were exposed to UV radiation 340 nm in a chamber prepared at the “Wood Protection Laboratory”, Facultad de Ciencias Forestales, Universidad de Concepción, Chile. The exposure chamber contained 4 UV tubes, 40 W (Q-Lab Corp., Cleveland, OH, USA), 48 inches length. Distance between exposed surfaces and tubes was kept on 50 mm and temperature and irradiation dose during the exposure were 40°C and 2.65 W/m^2 , respectively. Samples were randomly located on the exposure tray and randomly re-assorted every 200 h, until completing 2000 h of exposure.

2.5. Wood Surface Color Change Measurements

The color of wood samples exposed to artificial UV radiation was measured periodically. Samples were removed from the exposure chamber every 200 h during the first 1000 h of exposure, and then a final measurement was taken at the end of the exposure (2000 h). Color expressed in CIE $L^*a^*b^*$ coordinates was measured using a spectrophotometer Konica-Minolta CM-5. CIE $L^*a^*b^*$ color difference or color change (ΔE) was calculated for every sample by contrasting color measurements before and after exposure (Equation (1)).

$$\Delta E = [(L_2 - L_1)^2 + (a_2 - a_1)^2 + (b_2 - b_1)^2]^{1/2} \quad (1)$$

where:

L = lightness; a = greenness-redness; and b = yellowness-blueness.

Subscript (1) and (2) represented color reading before and after exposure, respectively.

2.6. Chemical Changes of Untreated Wood Surfaces

Fourier transform infrared spectroscopy–attenuated total reflectance (FTIR–ATR) was used to evaluate the effectiveness of the exposure setup prepared for this experiment. Wood samples, measuring 20 mm (width) \times 60 mm (length) \times 8 mm (thickness) were sawn from untreated samples,

before and after UV exposure, and stored for 5 days in a vacuum desiccator over silica gel. FTIR-ATR spectra of exposed surfaces were obtained using a single-bounce attenuated total reflectance accessory (Bruker Optic Pvt. Ltd., Billerica, MA, USA). Spectra of the fingerprint region 4000 to 400 (cm^{-1}) represented 36 accumulations at 4 cm^{-1} of resolution. Attempts to measure chemical changes by FTIR-ATR in treated samples were unsuccessful due to the intense reflect effect of the nanoparticles deposited onto the surface of the samples.

2.7. Transmission Electron Microscopy

Transmission electron microscopy (TEM) was used to examine the TiO_2 NP and TiO_2 -Si NP prior their use. TEM observations were made to resolution of 4 \AA in a JEOL-JEM 1200EX-II, Tokyo, Japan, transmission electron microscope.

2.8. Scanning Electron Microscopy

Scanning electron microscopy (SEM) was used to examine wood surfaces treated with TiO_2 NP and TiO_2 -Si NP after UV exposure. Small samples measuring $5 \times 5 \text{ mm}^2$, were cut from the parent sample and glued to aluminium stubs using nylon nail polish as an adhesive. The stubs containing the pieces of wood were stored for 5 days in a vacuum desiccator over silica gel. The stubs were coated with a 10 nm layer of gold using a sputter coater and then examined using a JSM-6380, Tokyo, Japan, scanning electron microscope, at an accelerating power of 20 W and a spot size of $40 \mu\text{m}$.

3. Results

The modification of TiO_2 NP with TEOS resulted in an increment in the size of the nanoparticles. The modification of NP with TEOS generate a silica cover layer, which can affect the photocatalytic activity of the nanoparticles [18]. The increment in the size of the nanoparticles was observed by TEM microscopy (Figure 1). The size of unmodified and modified TiO_2 NP, measured by image analysis, was $101 (\pm 12) \text{ nm}$, with a symmetrical distribution and $576 (\pm 43) \text{ nm}$ with a right-skewed distribution, respectively. In both cases, it was also observed that nanoparticles were prone to form aggregations. The presence of Si on modified nanoparticles was confirmed by energy-dispersive X-ray spectroscopy (EDS). Size distribution and EDS analyses are available as supplemented data. Nanoparticles modified with TEOS were called TiO_2 -Si NP. EPR spectroscopy revealed that TiO_2 NP were capable of generating important amounts of $\cdot\text{OH}$ radicals in the presence of UV light within the range of solar radiation (340 nm). The intensity of $\cdot\text{OH}$ radicals in TiO_2 NP increased over time, and the EPR signal was lower the limit of detection (LOD) at the beginning of reaction, increasing linearly to 6.4 (arbitrary units, a.u.), after 60 min of UV exposure. At the same sampling time and reaction conditions, the TiO_2 -Si NP showed activity under the LOD. In this way, the photoactivity was completely suppressed in TiO_2 -Si NP, demonstrating the effectiveness of the treatment with TEOS (Figure 2). A supplementary method was also used to test the photocatalytic effect of TiO_2 nanoparticles and the suppression of such effects due to the TEOS treatment. In a batch system, safranin and methylene blue solutions were exposed to UV radiation in the presence of TiO_2 and TiO_2 -Si NP, respectively. The experiment demonstrated the potential of the TiO_2 nanoparticles to induce photochemical changes in the presence of organic molecules, as the solutions containing unmodified nanoparticles were almost completely degraded after UV exposure. Conversely, the passivation of the TiO_2 -Si nanoparticles was also confirmed, as the solutions containing these nanoparticles remained practically undegraded after exposure (Supplementary Data).

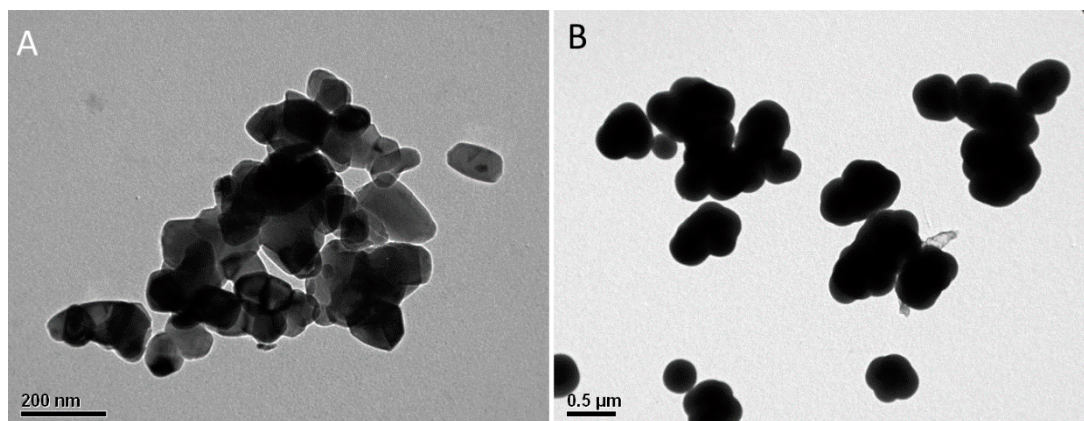


Figure 1. Transmission electron microscopy (TEM) images of TiO_2 unmodified (A) and modified nanoparticles (B). Size increment on modified nanoparticles can be attributable to the accumulation of a Silica on their surface.

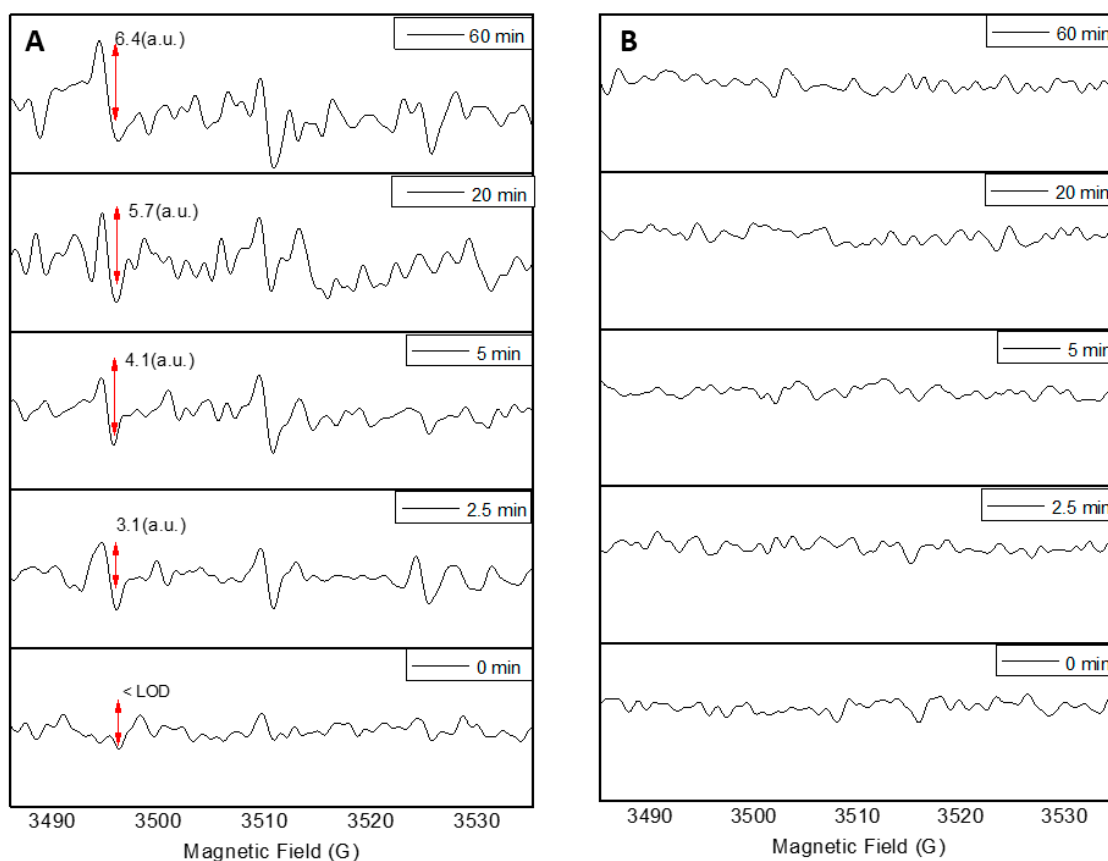


Figure 2. Intensity in arbitrary units (a.u.) of abstracted hydroxyl radicals (OH) produced by TiO_2 (A) and $\text{TiO}_2\text{-Si}$ (B) at different times of exposure to UV radiation, measured by electron paramagnetic resonance (EPR) spectroscopy. LOD (limit of detection).

On the other hand, EPR experiments on wood samples without spin trappings revealed the presence of a characteristic signal of uncoupled spin at control and nanoparticle-treated samples exposed to UV radiation (Figure 3). Based on the chemical changes detected in lignin by FTIR in control samples (Figure 4), this signal was attributed to the phenoxy radicals delocalized on the aromatic rings (uncouples spin) that are readily produced due to the photolysis of lignin under UV light [14,17,20]. FTIR-ATR test in control samples after UV exposure, showed an increment in the transmittance at wavelengths 1261 cm^{-1} , assigned to C–O stretching vibration in lignin [21] and

1508 cm^{-1} , assigned to aromatic skeletal vibrations lignin [21,22]. Conversely a decrease in the peaks at wavelengths 1611 cm^{-1} , assigned to C=C unsaturated linkages [23] and 1736 cm^{-1} , corresponding to C=O stretching, which occurs due to oxidative degradation by UV [24]. Pathways for lignin photo-oxidation involve several routes in which phenoxy radicals react with oxygen and other radicals in the system to generate the chromophore compounds responsible for the color change in wood surfaces in the presence of UV radiation [25–29].

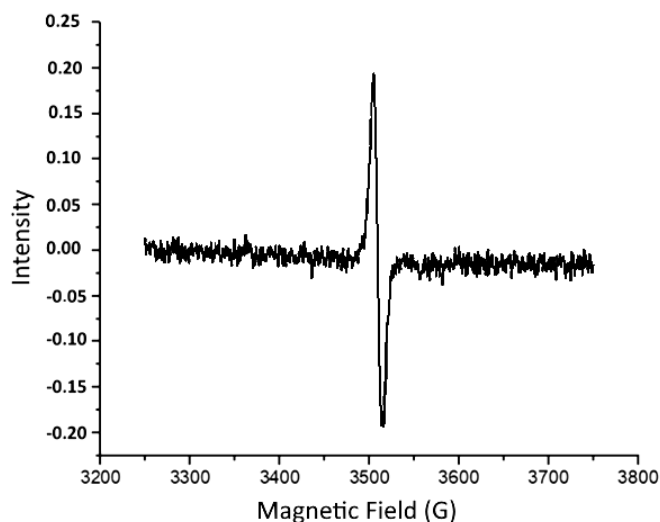


Figure 3. EPR radical signal detected in untreated wood samples, and treated with TiO_2 and $\text{TiO}_2\text{-Si}$, after 120 min of exposure to artificial UV radiation 340 nm.

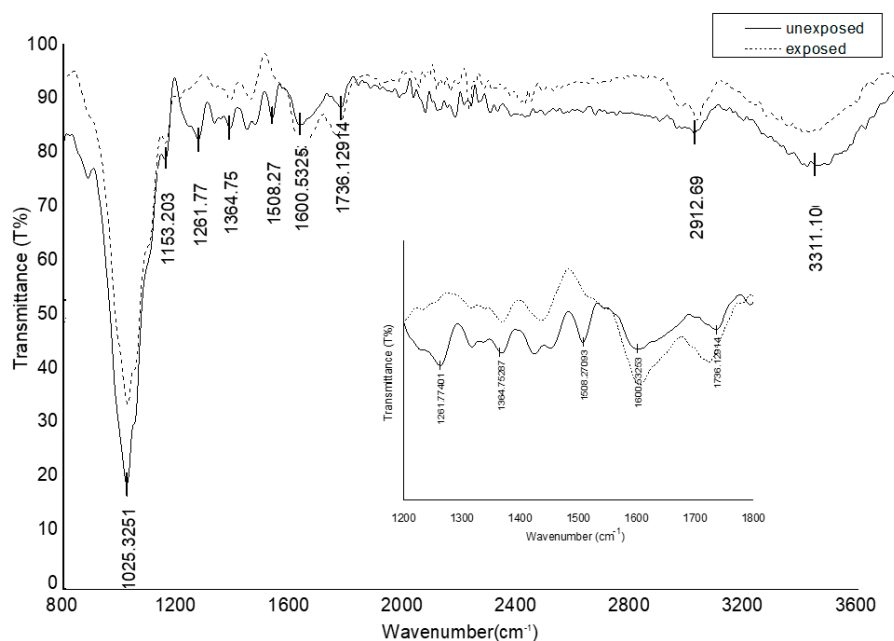


Figure 4. Normalized FTIR-ATR spectrum of control wood samples, exposed and unexposed to 2000 h of artificial UV radiation 340 nm.

In the wood samples, the intensity of the signal detected by EPR (quantitative EPR technique) was recorded after 120 min of UV exposure (Figure 5). Phenoxy radical intensity was considerably higher in control samples, showing the strong and well documented photo-oxidative effect of UV light over lignin [14]. However, this intensity decreased significantly in the presence of $\text{TiO}_2\text{-Si}$ nanoparticles and decreased even further in the presence of TiO_2 . These results were confirmed at long-term exposure, in an experiment that considered wood surface color changes as an indicator of chemical changes due

to photo-oxidative reactions. In this experiment, the analysis of variance showed a significant effect of the NP treatment used on the samples and the time of exposure (Table 1). The level of photoprotection provided by TiO_2 and $\text{TiO}_2\text{-Si}$ was noticeable in comparison to untreated control samples. Nevertheless, the level of protection of TiO_2 was always superior to $\text{TiO}_2\text{-Si}$, i.e., samples depicted always a lower color-change value, and the differences between both treatments increased significantly after 1000 h of exposure ($p\text{-value} < 0.05$) (Figure 6), hence demonstrating the superior performance of TiO_2 over $\text{TiO}_2\text{-Si}$ to decrease color changes in long-term UV exposure. SEM images of wood samples treated with TiO_2 and $\text{TiO}_2\text{-Si}$ nanoparticles showed that the treatment formed a discontinuous layer on the wood surfaces, with zones where the nanoparticles were completely absent and zones where they formed aggregations (Figure 7).

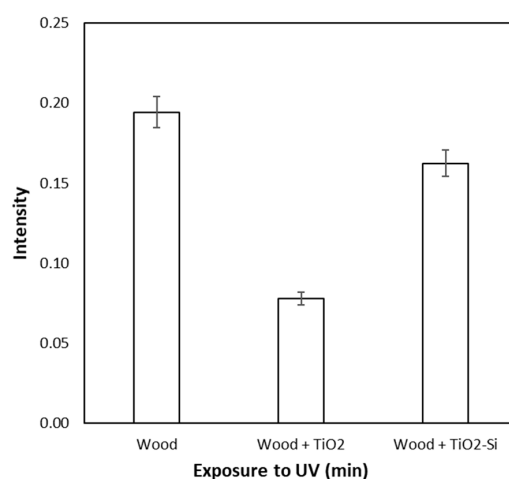


Figure 5. Intensity of EPR signal detected in wood samples treated with TiO_2 and $\text{TiO}_2\text{-Si}$, and untreated (control), after two hours of exposure to artificial UV radiation 340 nm.

Table 1. Effect (p -value) of nanoparticle, exposure time, and interaction between both factors, on the color change of wood samples treated with TiO_2 , $\text{TiO}_2\text{-Si}$, and untreated controls, exposed to artificial UV radiation 340 nm.

Factor	p -Value
A: Nanoparticle treatment	
B: Time of exposure	
A \times B	<0.0001

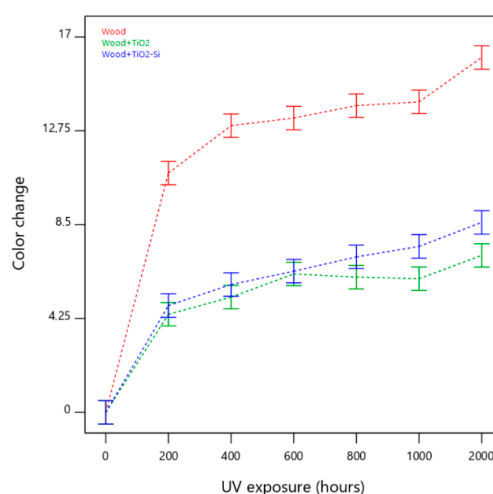


Figure 6. Color change of wood surfaces treated with TiO_2 (Wood + TiO_2), $\text{TiO}_2\text{-Si}$ (Wood + $\text{TiO}_2\text{-Si}$) and untreated control (wood), after 2000 h of exposure to artificial UV radiation 340 nm.

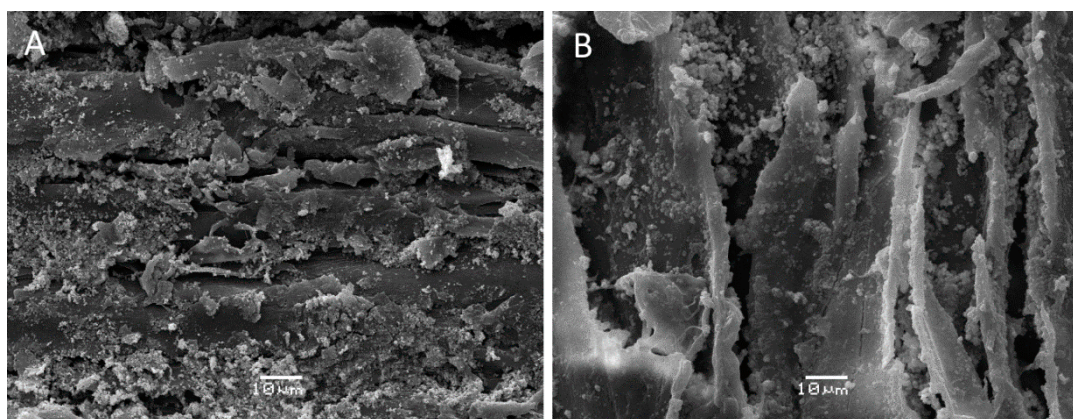


Figure 7. Scanning electron microscopy (SEM) images of TiO_2 treated wood surfaces. (A) surface treated with unmodified nanoparticles and (B) surface treated with modified nanoparticles.

4. Discussion

In this work, we focused our attention on the photoactivity of TiO_2 nanoparticles as a factor that may influence its performance as photoprotective treatment for wood surfaces. TiO_2 offers protection against UV radiation due to its ability to block, scatter and absorb UV radiation [3]. Nevertheless, the absorption of UV photons comprises the migration of electrons in the valence band towards the conduction band, creating holes that can migrate with the excited electrons to the surface of the nanoparticles [12,30]. In the presence of water and oxygen, these electrons and holes generate hydroxy and superoxide radicals that can readily interact with the electron donor and accept compounds in a process known as photocatalysis [5,7,31]. The photocatalytic effect of TiO_2 NP has been well documented in polymeric materials, in which the use TiO_2 NP with suppressed photocatalytic activity has resulted in improved photoprotection and increased lifetime of the product [3]. At wood surfaces, reports shown contradictory evidence. For instances, Rassam et al. [32] reported no damage due to deposited TiO_2 nanoparticles on wood surfaces after UV exposure, but Zheng et al. [33] described the peeling and degradation of wood surfaces and coatings because of the photocatalytic effect of TiO_2 nanoparticles. Our experimental results show that the suppression of photocatalytic activity, i.e., the use of TiO_2 -Si to treat wood surfaces, resulted in an increment in aromatic radicals and color changes at long-term UV exposure. This outcome, opposite to the original hypothesis of this study, may be explained by the ability of TiO_2 to act as an electron sink agent at its rutile phase. In the commercial preparation of TiO_2 , i.e., Degussa P25 rutile, acts as an electron sink agent extending the lifetime of trapped holes [34]. Under such a principle, the holes and excited electrons that migrated to the surface of the nanoparticles after the absorption of UV photons may be interacting with the aromatic radicals produced in wood, interrupting further oxidative reaction with other wood components (Figure 8), hence decreasing color changes at wood surfaces. For this hypothesis to occur, close contact of the nanoparticles with the substrate may be necessary, which is given due to the high surface area and size of the nanoparticles and the small, deep penetration of UV radiation on wood [35]. In support of this, SEM images revealed that the treated with TiO_2 and TiO_2 -Si nanoparticles formed a discontinuous layer at wood surfaces, with gaps where nanoparticles were absent and zones where they formed aggregations (Figure 7). This indicates that the mechanism of photoprotection may not be only associated with the blocking or scattering effect of the nanoparticles, but also with possible interactions between charged nanoparticles and the radical species produced at the wood surfaces, as evidently UV photons still could reach wood surfaces. Further testing is required to confirm these assumptions. These tests may include the use of nanoparticles with different levels of photoactivity and sizes; the quantification of the electron sink effect of these nanoproductions and the inclusion of chemical compounds that may act as a competitor against the aromatic radical formed in wood for the active sites on the photo-excited nanoparticles. In addition, the inclusion of other wood species for

testing could be implemented. Variations in lignin and extractives' composition and concentration can also affect the photo-degradation of wood surfaces, therefore leading to slightly different results in terms of color change.

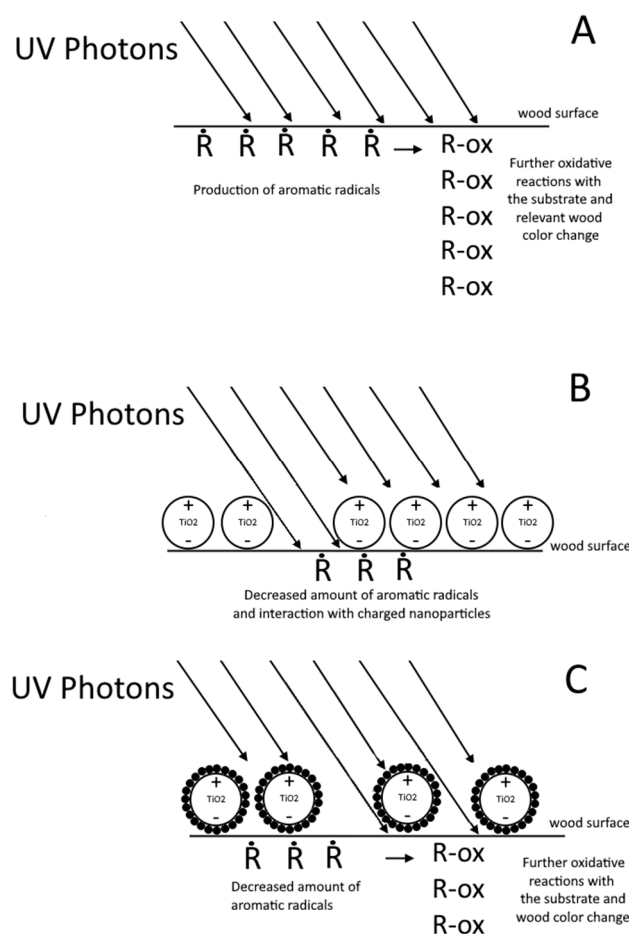


Figure 8. Scheme of action of TiO₂ on wood protection. (A) photo-oxidation of wood surfaces and aromatic radical production and oxidation leading to color change in wood surfaces. (B) action of TiO₂ nanoparticles blocking UV radiation and absorbing UV photons, where reduced amounts of aromatic radicals interact with charged nanoparticles, preventing further oxidative oxidation with the substrate. (C) modified TiO₂ nanoparticles; to reduce their photoactivity, aromatic radicals are prevented to interact with the charged nanoparticles, leading to further oxidative reaction with the substrate and color change in wood surfaces.

According to Hon et al. [13], photosensitizers and inorganic compounds in wood can be involved in the production of singlet oxygen, contributing in this way to the chemical changes that led to its discoloration. Similarly, hydroxy radicals have been regarded as one of the main non-enzymatic agents involved in the first stages of brown-rot decay and, to a lesser extent, they have also been detected during white-rot decay [15,16]. Considering this initial information, we selected a method consisting of the passivation of the nanoparticles with a silica cover layer to test whether the suppression of the hydroxy radical production influenced the level of photoprotection provided by the TiO₂ NP. Effects on the oxidation potential of Si modified rutile have been reported for the substitutional Si to O-doped TiO₂. Yang et al. [36] reported that, for this substitution, the Fermi level is pinned in the conduction band edge about 0.2 eV above the conduction band of pure rutile TiO₂. As the electron transition energy from the valence band to the conduction band above the Fermi level suggests a null decrease due to the counteraction, improved absorption of visible light is not expected [36]. In the case of substitutional Si- to Ti-doped rutile, Yang et al. reports that the valence band maximum has no shift,

while the conduction band bottom has a decline of about 0.2 eV, compared with that of pure rutile NPs. Therefore, a shift in absorption edge may also appear in the substitutional Si- to Ti-doped rutile TiO₂ [36,37]. Since the modification with Si implies no major changes in the oxidation potential of TiO₂, the role played by the Si as a physical barrier to avoid the interaction of radical species with the substrate takes relevance. In this work, such an effect was observed as a decrease in the intensity of OH radicals, measured by EPR, and the tapered capacity to degrade safranin and methylene-blue solutions in the presence of UV radiation by TiO₂-Si NP.

The photocatalytic effect of TiO₂ can be considered unimportant in certain materials, as the reduction in the number of active photons due to TiO₂ absorption may be more relevant than the photocatalytic effect of the nanoparticles [3]. Nevertheless, the results obtained in this work indicate that, for wood surfaces, the photocatalytic activity of the TiO₂ may be crucial in the performance of the photoprotective treatment.

5. Conclusions

It has been reported that the photocatalytic effect of TiO₂ NP can make a minor contribution to the photo-oxidation of different polymeric materials. However, when these nanoparticles are used to protect wood surfaces against UV radiation, such an effect is not often informed. In this work, we studied how the suppression of the photocatalytic activity of TiO₂ NP may influence the color change in wood surfaces after UV radiation. Experimental results showed that the addition of a silica layer onto the surface of the nanoparticles is effective at suppressing the photocatalytic activity of TiO₂. In addition, contrary to the initial hypothesis of this study, the use of TiO₂ with suppressed photoactivity was less effective at preventing color change than the treatment with photoactive TiO₂ nanoparticles. The results suggest that, for wood surfaces, the photocatalytic activity of the TiO₂ may be crucial on its performance as photoprotective treatment. Further experimentation is necessary to confirm this assumption; such experiments may include the testing of nanoparticles with different levels of photoactivity and the determination of their ability to act as an electron sink agent.

Supplementary Materials: The following are available online at <http://www.mdpi.com/2079-6412/10/11/1033/s1>, Table S1, Figures S1 and S2: determination of TiO₂ and TiO₂-Si nanoparticles size and distribution, Figures S3 and S4 showing degradation of safranin and methylene-blue in presence of TiO₂ and TiO₂-Si, EDS Analysis (Figures S5 and S6) of wood samples treated with TiO₂-Si and TiO₂.

Author Contributions: Conceptualization, V.H. and D.C.; methodology, V.H., N.S., G.P.-G., and C.M.; formal analysis, V.H., D.C., G.P.-G., and R.R.; writing—original draft preparation, V.H. and R.R.; writing—review and editing, V.H., D.C., and R.R.; supervision, V.H. and D.C. All authors have read and agreed to the published version of the manuscript.

Funding: This research was funded by ANID, Fondecyt 11180030.

Acknowledgments: V.H. acknowledge the support from PAI Convocatoria Nacional Subvención a Instalación en la Academia 2018, 77180054. D.C. and R.R. thanks the support from FONDAP Solar Energy Research Center ANID/FONDAP/15110019.

Conflicts of Interest: The authors declare no conflict of interest. The funder had no role in the design of the study; in the collection, analyses, or interpretation of data; in the writing of the manuscript, or in the decision to publish the results.

References

1. Fufa, S.; Jelle, B.; Hovde, P. Effects of TiO₂ and clay nanoparticles loading on weathering performance of coated wood. *Prog. Org. Coat.* **2013**, *76*, 1425–1429. [[CrossRef](#)]
2. Zanatta, P.; Lazarotto, M.; Gonzalez de Cademartori, P.; Cava, S.; Moreira, M.; Gatto, D. The effect of titanium dioxide nanoparticles obtained by microwave-assisted hydrothermal method on the color and decay resistance of pinewood. *Maderas Cienc. Tecnol.* **2017**, *19*, 495–506. [[CrossRef](#)]
3. Egerton, T. UV-Absorption—The primary process in photocatalysis and some practical consequences. *Molecules* **2014**, *19*, 18192–18214. [[CrossRef](#)] [[PubMed](#)]

4. Evans, P. Weathering and Photoprotection of Wood. In *Development of Commercial Wood Preservatives*; ACS Symposium Series; American Chemical Society: Washington, DC, USA, 2008; Volume 982, pp. 69–117.
5. Beydoun, D.; Amal, R.; Low, G.; McEvoy, S. Role of nanoparticles in photocatalysis. *J. Nanoparticle Res.* **1999**, *1*, 439–458. [[CrossRef](#)]
6. Brezová, V.; Gabčová, S.; Dvoranová, D.; Staško, A. Reactive oxygen species produced upon photoexcitation of sunscreens containing titanium dioxide (an EPR study). *J. Photochem. Photobiol. B* **2005**, *79*, 121–134. [[CrossRef](#)] [[PubMed](#)]
7. Gladis, F.; Schumann, R. A suggested standardised method for testing photocatalytic inactivation of aeroterrestrial algal growth on TiO₂-coated glass. *Int. Biodeterior. Biodegrad.* **2011**, *65*, 415–422. [[CrossRef](#)]
8. Jain, A.; Vaya, D.; Jain, A.; Vaya, D. Photocatalytic activity of TiO₂ nanomaterials. *J. Chil. Chem. Soc.* **2017**, *62*, 3683–3690. [[CrossRef](#)]
9. Nevárez-Martínez, M.; Espinoza-Montero, P.; Quiroz-Chávez, F.; Ohtani, B. Fotocatálisis: Inicio, actualidad y perspectivas a través del TiO₂. *Av. Quím.* **2017**, *12*, 45–59.
10. Hughes, W. *Photodegradation of Paint Films Containing TiO₂ Pigments*; Verlag Chemie GmbH: Weinheim/Bergst, Germany, 1970; pp. 67–82.
11. Allen, N.; McKellar, J.; Phillips, G.; Chapman, C. The TiO₂ photosensitized degradation of nylon 6, 6: Stabilizing action of manganese ions. *J. Polym. Sci. Lett.* **1974**, *12*, 723–727. [[CrossRef](#)]
12. Tsuzuki, T.; He, R.; Wang, J.; Sun, L.; Wang, X.; Hocking, R. Reduction of the photocatalytic activity of ZnO nanoparticles for UV protection applications. *Int. J. Nanotechnol.* **2012**, *9*, 1017–1029. [[CrossRef](#)]
13. Hon, D.; Chang, S.; Feist, W. Participation of singlet oxygen in the photodegradation of wood surfaces. *Wood Sci. Technol.* **1982**, *16*, 193–201. [[CrossRef](#)]
14. Baur, S.; Easteal, A. ESR studies on the free radical generation in wood by irradiation with selected sources from UV to IR wavelength regions. *Holzforschung* **2014**, *68*, 775–780. [[CrossRef](#)]
15. Backa, S.; Gierer, J.; Reitberger, T.; Nilsson, T. Hydroxyl radical activity in brown-rot fungi studied by a new chemiluminescence method. *Holzforschung* **1992**, *46*, 61–67. [[CrossRef](#)]
16. Tanaka, H.; Itakura, S.; Enoki, A. Hydroxyl radical generation by an extracellular low-molecular-weight substance and phenol oxidase activity during wood degradation by the white-rot basidiomycete *Trametes versicolor*. *J. Biotechnol.* **1999**, *75*, 57–70. [[CrossRef](#)]
17. Hon, D.; Ifju, G.; Feist, W. Characteristics of free radicals in wood. *Wood Fiber* **1980**, *12*, 121–130.
18. Chia, S.; Leong, D. Reducing ZnO nanoparticles toxicity through silica coating. *Heliyon* **2016**, *2*, e00177. [[CrossRef](#)]
19. Yamazaki, I.; Piette, L. ESR spin-trapping studies on the reaction of Fe²⁺ ions with H₂O₂-reactive species in oxygen toxicity in biology. *J. Biol. Chem.* **1990**, *265*, 13589–13594. [[PubMed](#)]
20. Hon, D.; Ifju, G. Measuring penetration of light into wood by detection of photo-induced free radicals. *Wood Sci.* **1978**, *11*, 118–127.
21. Faix, O. Classification of lignins from different botanical origins by FT-IR spectroscopy. *Holzforschung* **1991**, *45*, 21–28. [[CrossRef](#)]
22. Harrington, K.; Higgins, H.; Michell, A. Infrared spectra of *Eucalyptus regnans* F. Muell and *Pinus radiata* D. Don. *Holzforschung* **1964**, *18*, 108–113. [[CrossRef](#)]
23. Chazal, R.; Robert, P.; Durand, S.; Devaux, M.; Saulnier, L.; Lapierre, C.; Guillon, F. Investigating lignin key features in maize lignocelluloses using infrared spectroscopy. *Appl. Spectrosc.* **2014**, *68*, 1342–1347. [[CrossRef](#)]
24. Lionetto, F.; Del Sole, R.; Cannoletta, D.; Vasapollo, G.; Maffezzoli, A. Monitoring wood degradation during weathering by cellulose crystallinity. *Materials* **2012**, *5*, 1910–1922. [[CrossRef](#)]
25. Kringstad, K.; Lin, S. Mechanisms in the yellowing of high yield pulps by light: Structure and reactivity of free radical intermediates in the photodegradation of lignin. *Tappi* **1970**, *53*, 2296–2301.
26. Gierer, J.; Lin, S. Photodegradation of lignin. A contribution to the mechanism of chromophore formation. *Sven Papp.* **1972**, *75*, 233–239.
27. Scaiano, J.; Netto-Ferreira, J.; Wintgens, V. Fragmentation of ketyl radicals derived from α -phenoxyacetophenone: An important mode of decay for lignin-related radicals? *J. Photochem. Photobiol. Chem.* **1991**, *59*, 265–268. [[CrossRef](#)]
28. Schmidt, J.; Heitner, C. Light-induced yellowing of mechanical and ultrahigh yield pulps. Part 2. Radical-induced cleavage of etherified guaiacylglycerol- β -arylether groups is the main degradative pathway. *J. Wood Chem. Technol.* **1993**, *13*, 309–325. [[CrossRef](#)]

29. Schaller, C.; Rogez, D. New approaches in wood coating stabilization. *J. Coat. Technol. Res.* **2007**, *4*, 401–409. [[CrossRef](#)]
30. Mills, A.; Le Hunte, S. An overview of semiconductor photocatalysis. *J. Photochem. Photobiol. Chem.* **1997**, *108*, 1–35. [[CrossRef](#)]
31. Mahmoodi, N.; Arami, M.; Limaee, N.; Tabrizi, N. Kinetics of heterogeneous photocatalytic degradation of reactive dyes in an immobilized TiO₂ photocatalytic reactor. *J. Colloid Interface Sci.* **2006**, *295*, 159–164. [[CrossRef](#)]
32. Rassam, G.; Abdi, Y.; Abdi, A. Deposition of TiO₂ nano-particles on wood surfaces for UV and moisture protection. *J. Exp. Nanosci.* **2012**, *7*, 468–476. [[CrossRef](#)]
33. Zheng, R.; Tshabalala, M.; Wang, H. Photocatalytic degradation of wood coated with a combination of rutile TiO₂ nanostructures and low-surface free-energy materials. *Bioresources* **2016**, *11*, 2393–2402. [[CrossRef](#)]
34. Hurum, D.; Agrios, A.; Gray, K.; Rajh, T.; Thurnauer, M. Explaining the enhanced photocatalytic activity of Degussa P25 mixed-phase TiO₂ Using EPR. *J. Phys. Chem. B* **2003**, *107*, 4545–4549. [[CrossRef](#)]
35. Kataoka, Y.; Kiguchi, M.; Evans, P. Photodegradation depth profile and penetration of light in Japanese cedar earlywood (*Cryptomeria japonica* D. Don) exposed to artificial solar radiation. *Surf. Coat. Int. Part B Coat. Trans.* **2004**, *87*, 149–234. [[CrossRef](#)]
36. Yang, K.; Dai, Y.; Huang, B. First-principles calculations for geometrical structures and electronic properties of Si-doped TiO₂. *Chem. Phys. Lett.* **2008**, *456*, 71–75. [[CrossRef](#)]
37. Long, R.; Dai, Y.; Meng, G.; Huang, B. Energetic and electronic properties of X- (Si, Ge, Sn, Pb) doped TiO₂ from first-principles. *Phys. Chem. Chem. Phys.* **2009**, *11*, 8165–8172. [[CrossRef](#)]

Publisher's Note: MDPI stays neutral with regard to jurisdictional claims in published maps and institutional affiliations.



© 2020 by the authors. Licensee MDPI, Basel, Switzerland. This article is an open access article distributed under the terms and conditions of the Creative Commons Attribution (CC BY) license (<http://creativecommons.org/licenses/by/4.0/>).